The hippocampal formation mapped in the BigBrain:
The deep-learning supported high-resolution mapping and 3D reconstruction

Olga Kedo[1*], Kimberley Lothmann[1,3*], Christian Schiffer[1,2*], Hartmut Mohlberg[1], Timo Dickscheid[4,1,2], Katrin Amunts[1,3]

o.kedo@fz-juelich.de

[1] Institute for Neuroscience and Medicine (INM-1), Research Centre Jülich, Germany
[2] Helmholtz AI, Research Centre Jülich, Jülich, Germany
[3] C. & O. Vogt Institute for Brain Research, Medical Faculty, University Hospital Düsseldorf Heinrich-Heine-University
[4] Institute of Computational Visualistics, University of Koblenz, Koblenz, Germany

The hippocampal formation (HF) plays a pivotal role in different aspects of memory, with its subdivisions being involved in different functions and neuropathologies [1-3]. The heterogeneous architecture of the areas led to different parcellation schemes both in histological and MRI studies [4-5], with different number of structures analyzed. In the BigBrain, unfolding and unsupervised clustering of laminar and morphological features revealed main structures of the hippocampus [6]. Previously, we have mapped 11 areas of the hippocampus, including areas of the dentate gyrus, Cornu ammonis and subicular complex, hippocampal-amygdaloid transition area and transsubiculum, based on differences in receptor- and in cytoarchitecture, and probabilistic maps were created based on the analysis of 10 postmortem brains [7]. Here we build on this research, and generate the high-resolution anatomical reference of the entire HF in the BigBrain template, including the entorhinal cortex [8] to enrich the map, considering its interconnectivity with the hippocampus in the memory. Volume comparison of the HF in the BigBrain vs. previously mapped 10 brains revealed a typical structure of all areas of the HF of the BigBrain, except for PaS.

Methods Cytoarchitectonic mapping was performed in serial, coronal, cell body-stained sections (Fig. 1 A-B) in both hemispheres. We examined the hippocampal formation (Fig.1C) in histological sections at 1 micron resolution of the BigBrain. Structures were identified and manually delineated at least in each 15th section at 20 micron resolution in-plane in OnlineSectionTracer in 10 brains. All manual delineations were transformed in the web-based annotation tool (MicroDraw: The Institut Pasteur, Paris, France, https://github.com/r03ert0/microdraw) at 1 micron resolution in-plane.

Fig. 1 Cytoarchitecture of the hippocampal formation (HF) Structures of the HF were cytoarchitectonically identified in the BigBrain (**A, B**). The hippocampus represented by Cornu ammonis CA1 – CA3 and FD belong to the 3-layered allocortex (**C**). CA4 is surrounded by FD within the dentate gyrus. SubC included both allocortical (ProS and Sub) and periallocortical (PreS, PaS) structures (**C**). ProS and Sub reveal sublayers within their pyramidal cell layer 2 (**C**). All structures of the HF are heterogeneous, rostro-caudally and medio-laterally. Allocortical HATA and periallocortical TrS represent transition to the amygdala (**A**) and lateral periallocortex, area 35 (**B**)/proisocortex, respectively. Entorhinal cortex has most complex layering pattern, having 6 layers (**C**).

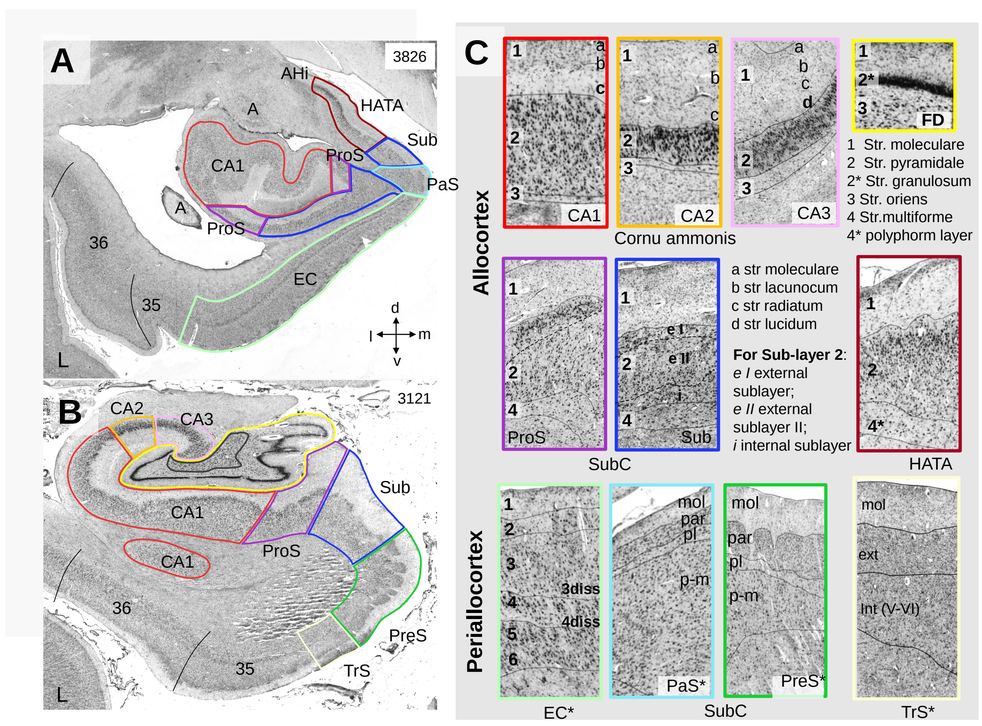

A amygdala, AHi amygdalo-hippocampal transition area, DG dentate gyrus, FD fascia dentata, EC entorhinal cortex, HATA hippocampal-amygdaloid transition area, PreS presubiculum, PaS parasubiculum, SubC subicular complex, TrS transsubiculum, L left hemisphere. *EC layers: 1 Str moleculare, 2 Str stellare, 3 Str pyramidale and substratum dissecantia (3diss), 4 str magnocellulare, 5 Str parvopyramidale, 6 Str multiforme; PaS layers: **mol** Str moleculare, **par** Str parvopyramidale, **pl** Str plexiforme, **p-m** Str pyramidale and multiforme. TrS* layers: **ext** external (overlap of periallocortical and proisocortical layers), **int** internal; d dorsal, v ventral, m medial, l lateral.
In the pyramidal layer of the ProS and Sub, sublayers are delineated by dotted lines.

Fig. 2 Macroanatomy of the HF based on the BigBrain The most caudal HF was located on the subsplenial gyrus, and was connected to Indusium griseum (IG, mapped only partly). TrS and caudal PreS was associated with the lateral wall of the isthmus (Ist) and caudal parahippocampal gyrus (PhG). TrS abutted on PreS ventrally, while rostral TrS abutted upon area 35. Caudally, PreS occupied medial surface of the PHG, while rostrally it was hidden in the uncal sulcus. PaS replaced TrS rostrally. Fasciola cinerea (fc, which is FD in its mediocaudal extension) was minuscule in its caudal aspect. The right ProS almost does not appear on the surface. PaS replaced TrS rostrally, on the free surface of the parahippocampal gyrus, but the rostral PaS was the most medial parahippocampal structure within the uncal sulcus. Rostrally, both hemispheres had three Digitationes hippocampi respectively. The area 35, 36 surround EC laterally; 36 is a border area towards the isocortex on the fusiform gyrus rostrally and parahippocampal gyrus caudally.

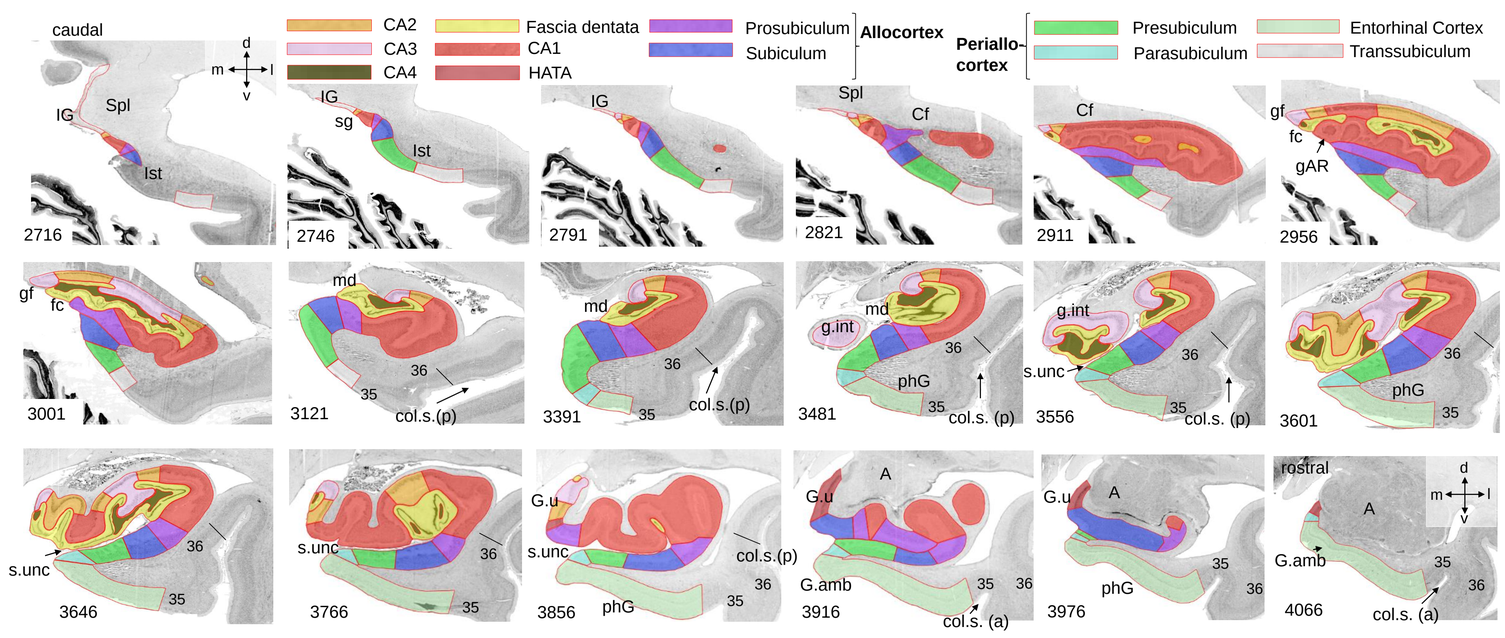

A amygdala, Cf Crus of fornicis, col.s (a) collateral sulcus (anterior segment), col.s (p) collateral sulcus (posterior segment), fc Fasciola cinerea, gAR Gyrus of Andreas Retzius, g.int Gyrus intralimbicus, gf Gyrus fasciolaris, G.u Gyrus uncinatus, IG Induseum griseum, Ist Isthmus, md Margo denticulatus, sg subsplenial gyrus, Spl Splenium, s.unc Sulcus uncinatus, d dorsal, v ventral, m medial, l lateral.

Methods We trained **multi-scale Convolutional Neural Networks (CNNs)** for image segmentation [9] in the unlabelled sections, separately for each data set, using ATLaSUI. Training and subsequent prediction of contour lines were performed on the supercomputer JURECA-DC at Jülich Supercomputer Centre [10]. Automatically generated predictions were checked for quality in MicroDraw, with low quality predictions being replaced by linear interpolations. All annotations were non-linearly transformed into the 3D reconstructed BigBrain space, surfaces were computed, and subdivisions were visualized using the Neuroglancer (Fig.4) [11].

Fig. 3 Comparison of delineations: Kedo et al. (A) with manual segmentations of deKraker et al. [6] (B)

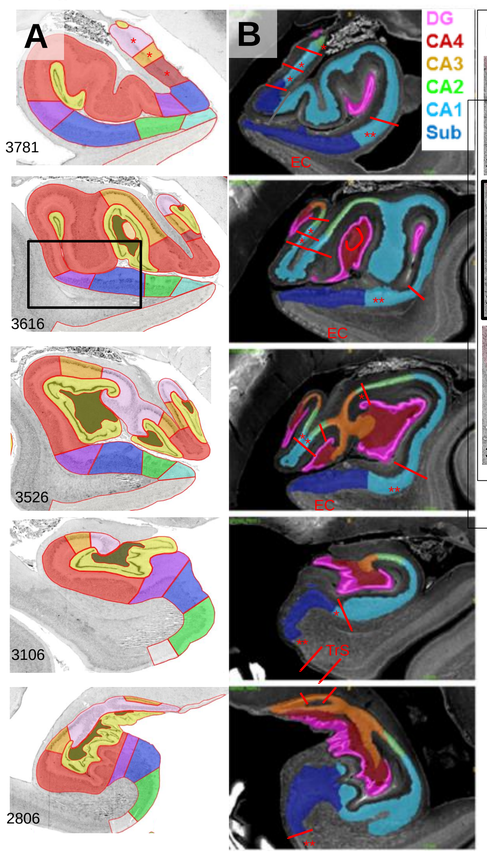

Methods
Manual segmentations are overlaid in the images to the right (B). Images iwere taken from coronal slices 716, 632, 590, 376, and 230 of the 40 µm native space left hippocampal block.
Red borders and asterisks are used to hightlight differences in border/area assignemnt.

Most discrepancy was found at the level of the hippocampal head,
- **CA1/ProS** border
(visualization of our criteria is in Fig.**3C**);

- areas located **dorsally on the Gyrus uncinatus** (at the level of caudal appearance of HATA)

- Less structures (not included TrS, EC, subdivision of SubC)

Motivation for more detailed comparison in the same BigBrain space

Fig. 4 3D reconstruction of the HF demonstrates relationships between the structures and their macroanatomic locations from the side view (**A**) and dorsal view (**B**), as well as relationship between the periallocortical structures (**C**). In the right hemisphere, EC is more rostrally extensive than on the left (**B**). The right medial internal Digitation hippocampi (**B***) is narrower than that in the left hemisphere. ProS is hidden in the hippocampal sulcus (hip.s), while the left ProS extends onto the dorsomedial surface of the PhG. Fasciola cinerea (FD in its mediocaudal extension) was larger in the left hemisphere (**A**). Caudally, PreS occupies medial surface of the PHG. TrS abuts on PreS ventrally (**A**).

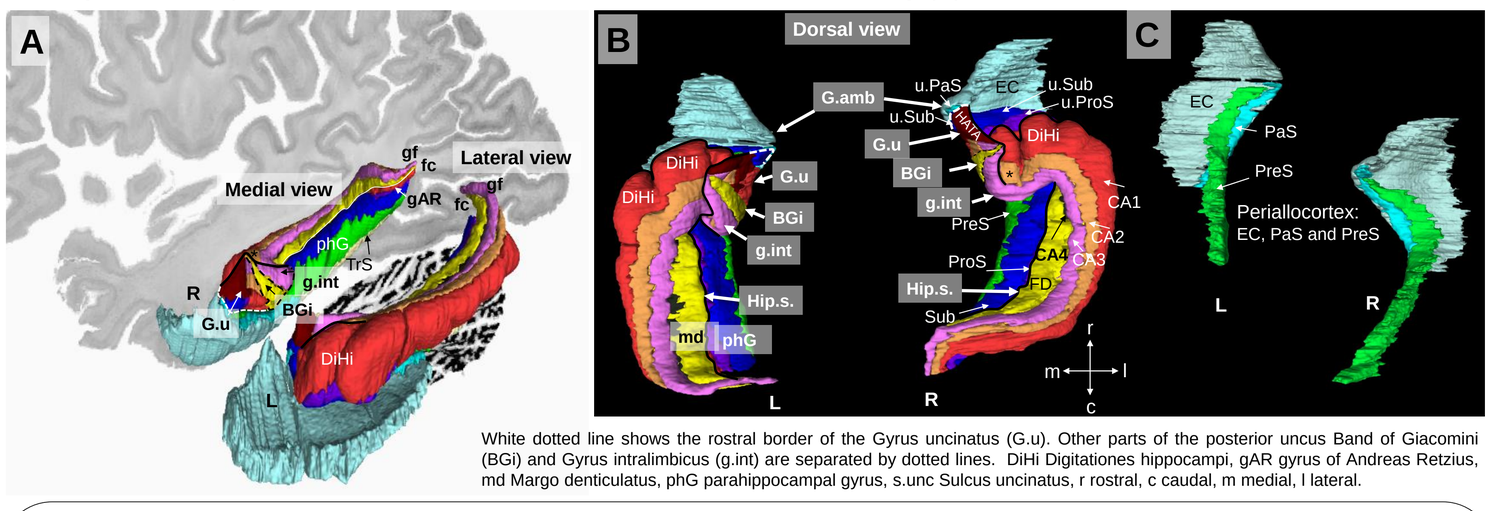

White dotted line shows the rostral border of the Gyrus uncinatus (G.u). Other parts of the posterior uncus Band of Giacomini (BGi) and Gyrus intralimbicus (g.int) are separated by dotted lines. DiHi Digitationes hippocampi, gAR gyrus of Andreas Retzius, md Margo denticulatus, phG parahippocampal gyrus, s.unc Sulcus uncinatus, r rostral, c caudal, m medial, l lateral.

Fig.5 Comparison of volumes of the areas of the HF in the BigBrain and in the postmortem brains [7] reveals a typical structure of the HF of the BigBrain, except for its smaller PaS.

Methods Manual delineations were used for the computation of volumes of the individual hippocampal areas using Cavalieri's principle [12]

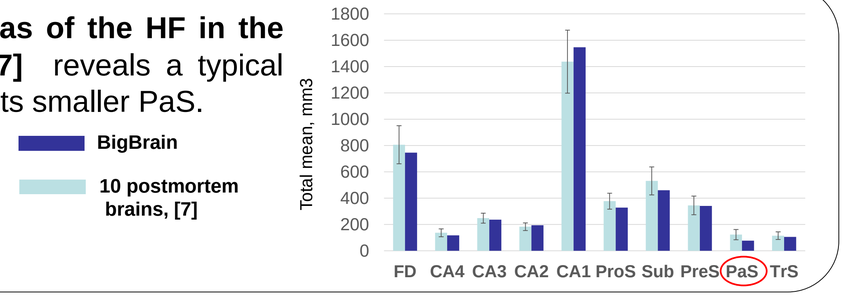

The hippocampal formation is a complex of structures, with several areas, each of which being involved in different aspects of memory or in neurodegeneration in different pathologies. Here we present the 3D high-resolution maps of the HF, based on the established parcellation scheme [7]. The maps will be publicly available on the EBRAINS platform and integrated with the BigBrain model (https://go.fzj.de/bigbrain/). These maps of the HF can extend those of the piriform cortex in the BigBrain [13] to represent two hubs of limbic system [14].

[1] Insausti R. et al (2023), The CA2 hippocampal subfield in humans: A review. *Hippocampus*, **vol. 33,** no. 6, pp. 712-9.
[2] Bakker A. et al. (2008), Pattern separation in the human hippocampal CA3 and dentate gyrus. *Science*, **vol. 319**, no. 5870, pp. 1640-2.
[3] Zeidman P. et al (2015), Investigating the functions of subregions within anterior hippocampus. *Cortex*, **vol. 73**, pp. 240-56.
[4] Wisse L. et al. (2017), A harmonized segmentation protocol for hippocampal and parahippocampal subregions: Why do we need one and what are the key goals? *Hippocampus*, **vol. 27,** no. 1, pp. 3-11.
[5] Yushkevich P. et al. (2015), Quantitative comparison of 21 protocols for labeling hippocampal subfields and parahippocampal subregions in in vivo MRI: towards a harmonized segmentation protocol. *Neuroimage*, **vol. 111**, pp. 526-41.
[6] DeKraker J. et al. (2020), Hippocampal subfields revealed through unfolding and unsupervised clustering of laminar and morphological features in 3D BigBrain. *Neuroimage*, **vol. 206**, p. 116328.
[7] Palomero-Gallagher N. et al. (2020), Multimodal mapping and analysis of the cyto- and receptorarchitecture of the human hippocampus. *Brain Struct Funct*, **vol. 225,** no. 3, pp. 881-907
[8] Amunts K. et al. (2013), BigBrain: an ultrahigh-resolution 3D human brain model, *Science*, **vol. 340,** no. 6139, pp. 1472-5
[9] Schiffer C. et al. (2021), Convolutional neuronal networks for cytoarchitectonic brain mapping at large scale, *Neuroimage*, **vol. 240**: p. 118327
[10] Krause D. and Thörnig P (2018), JURECA: Modular supercomputer at Jülich Supercomputing Centre, *J Large Scale Res. Facil.*, **vol. 4**, A132
[11] Gui X. et al. (2023) siibra-explorer – Interactive web viewer for multilevel brain atlases. Published online, April 19, 2023 *doi: 10.5281/zenodo.7885733*
[12] Amunts K. et al (2005), Cytoarchitectonic mapping of the human amygdala, hippocampal region and entorhinal cortex: intersubject variability and probability maps. *Anat Embryol,* **vol. 210**, no.5–6, pp. 343–352
[13] Kedo O. et al.(2024), Cytoarchitectonic Analysis and 3D Maps of the Mesial Piriform Region in the Human Brain. *Anatomia*, **vol. 3**, no. 2, p. 68–92. [**14**] Catani M. et al (2013), A revised limbic system model for memory, emotion and behaviour. *Neurosci Biobehav Rev*, **vol. 37**, no. 8, pp. 1724-37

This project received funding from the European Union's Horizon 2020 Research and Innovation Programme, grant agreement 945539 (HBP SGA3), and Special grant agreement 101147319 (EBRAINS 2.0 Project), from the Helmholtz Association's Initiative and Networking Fund through the Helmholtz International BigBrain Analytics and Learning Laboratory (HIBALL) under the Helmholtz International Lab grant agreement InterLabs-0015, from the Joint Lab SMHB. Computing time was granted through JARA on the supercomputer JURECA-DC at Jülich Supercomputing Centre (JSC).